

# Modeling Transport, Impact, and Spreading of Thermally Sprayed Polymer Particles

*R. A. Cairncross\**, *M. Ivosevic\*\** and *R. Knight\*\**

*\*Department of Chemical Engineering, Drexel University, Philadelphia, USA*

*\*\*Department of Materials Science and Engineering, Drexel University, Philadelphia, USA*

## Abstract

During thermal spray deposition, jets of high temperature and high velocity gases are used to accelerate and melt materials injected into the jet and propel them towards the surface to be coated. Upon impact at the surface, multiple hot particles deform, cool and consolidate to form a coating. Mathematical models have been developed to predict the particle transport and deformation on impact with a flat substrate during the High Velocity Oxy-Fuel (HVOF) combustion spraying of polymeric materials. The models of particle acceleration and heating in an HVOF jet are fully coupled and simultaneously integrated within the same FORTRAN code in order to predict particle velocity and temperature profiles at impact. A volume-of-fluid computational fluid mechanics package, Flow-3D<sup>®</sup>, was used to predict splat shapes using results from the acceleration and heating models as initial conditions. The predicted shapes of deformed particles exhibited good qualitative agreement with experimentally observed splats. Most of the experimentally observed Nylon 11 splats sprayed onto a room temperature substrate exhibited a characteristic “fried-egg” shape with a large, nearly-hemispherical, core in the center of a thin disk. This shape was formed by polymer particles having a low temperature, high viscosity core and a high temperature, low viscosity surface.

## 1. Introduction

*Thermal spray* is the generic term for the family of processes in which various materials are applied to form coatings, typically for corrosion, wear or thermal protection [1, 2]. The majority of thermal spray processes use thermal and kinetic energy (combustion flames, electric arcs or plasma jets) to melt and accelerate injected materials in powder or wire form. The resulting molten, or nearly molten, droplets/particles are accelerated in a gas stream to velocities in the range 50 to >1000 m/s and propelled against the surface to be coated. Upon impact at the surface they spread (splat), consolidate and cool (solidify) to form a coating or material deposit. Although thermal spraying is primarily used for the deposition of metals, ceramics and cermets, in recent years several authors have also reported successful deposition of both thermoset and thermoplastic polymers [3 - 7]. The advantages of using thermal spray processes for the deposition of polymers include: (i) solventless deposition of a coating without the use of volatile organic compounds (VOCs); (ii) the ability to coat large objects under almost any environmental conditions; (iii) the ability to apply polymer coatings with high melt viscosity; and (iv) the ability to produce “ready-to-use” coatings with limited need for post-deposition processing such as oven drying or curing, as is typically needed for electrostatic powder coatings and solvent-based paints. Disadvantages include: (i) lower deposition efficiency, (ii) lower quality surface finish and (iii) higher process complexity, often with narrow processing windows defined by the polymer melting and degradation temperatures.

Both mathematical modelling and experimental observations were correlated to better understand transport and splat formation of nylon 11 particles during high velocity oxy-fuel (HVOF) thermal spray process (Figure 1). The HVOF thermal spray process was selected due to the significantly higher gas speeds (> 1000 m/s) relative to other combustion driven thermal spray processes. For comparison, flame spray has slower gas speeds (< 200 m/s) and is also used for the deposition of polymers. The ability to accelerate particles to higher speeds is important for the deposition of materials with high melt viscosity, including high molecular

weight polymers and polymer/ceramic composites with high ( $> 5$  vol.%) ceramic reinforcement contents.

The unit process of thermal spraying is an individual droplet or particle impacting onto a substrate to form a splat. Coating characteristics such as porosity, roughness, adhesive and cohesive strengths depend on the morphology of these splats and how they bond to the substrate and to each other. As a result, many studies have examined droplet impact behavior in order to better understand and improve coating processes as summarized in the review papers by Sobolev and Guilemany [8], and Fauchais et al. [9]. Virtually all of the literature on modeling splatting in thermal spray, however, has focused on metallic particles. Although in principal similar, the heating and splatting behavior of polymer particles are fundamentally different owing to:

- Different flow characteristics of molten polymers versus those of metals
- Significantly different thermal properties and solidification kinetics

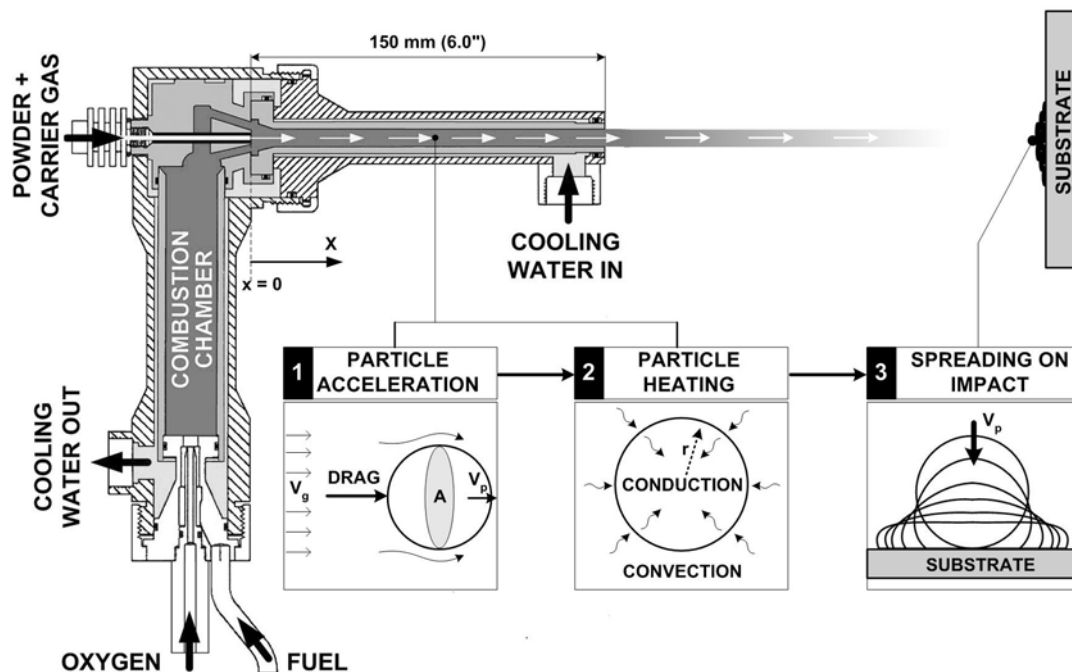


Figure 1. Schematic of Jet-Kote II<sup>®</sup> - high velocity oxy-fuel (HVOF) thermal spray gun and three main modeling steps (modified from the Stellite's Jet-Kote II<sup>®</sup> technical documentation).

The objectives of the research presented in this paper were: (i) to improve the qualitative understanding of acceleration and heating behavior of nylon 11 particles during HVOF spraying using both experiments and numerical modeling, (ii) to study the effect of different particle sizes and temperature gradients developed during particle acceleration in HVOF jets on splat formation process, (iii) to compare predicted splat shapes with experimental observations. These objectives will help to improve the understanding of the relationships between processing conditions, splat shapes and coating microstructures of HVOF sprayed polymers.

## 2. Mathematical Modeling

The unit operation of thermal spraying consists of:

- i. Delivering a particle to the gun
- ii. Accelerating and heating of the particle in the jet

- iii. Splating of the particle on impact with the substrate
- iv. And in some cases, post deposition flow of splats as a result of substrate preheating,

heating from the jet, or a subsequent heat treatment. Coatings are formed by the deposition and consolidation of many particles, a subject that will be covered in future publications.

In this paper mathematical modeling will be used to predict the three key steps shown in Figure 1: (1) particle acceleration, (2) particle heating and (3) spreading upon impact with a substrate. Particle acceleration and heating (steps 1 and 2) are fully coupled and were integrated simultaneously within the same FORTRAN code based on gas flow and thermal characteristics inside the HVOF gun. The particle velocity and internal temperature profile at impact were then used as initial conditions for modeling the particle impact and deformation on a flat substrate.

## 2.1 HVOF Gas Flow and Thermal Fields

The combustion and exhaust gas characteristics inside the HVOF gun are essential for modeling momentum and heat transfer to a particle (Figure 1 – steps 1 and 2). These characteristics were determined based on calculations published by Dobbins et al. [10] using the same HVOF system (Jet-Kite II<sup>®</sup>) as described in this paper. These conditions, together with the gun internal geometry, were used to estimate a maximum jet velocity of  $V_g^* \sim 800$  m/s (Mach  $\sim 0.6$ ) and temperature of  $T_g^* \sim 2000$  K. The mean axial gas temperature and velocity profiles were modeled based on an empirical correlation proposed by Tawfik et al. [11].

## 2.2 Particle Transport

The particle velocity and internal temperature profile at the moment of impact with the substrate are key inputs for determining the spreading behavior of impacting droplets. These were computed using momentum and heat transfer equations for particles in the HVOF flow field. It is commonly accepted [12] that the drag force is the dominant force governing the movement of particles in an HVOF jet, so that particle motion can be described by the following two ordinary differential equations:

$$m_p \frac{d\mathbf{v}_p}{dt} = \frac{1}{2} C_D \rho_g A_p (\mathbf{v}_g - \mathbf{v}_p) |\mathbf{v}_g - \mathbf{v}_p|, \quad \mathbf{v}_p(0) = 0, \quad (1)$$

$$\frac{dx}{dt} = \mathbf{v}_p, \quad x(0) = 0$$

Here ( $V_p$ ) is the particle axial velocity, ( $A_p$ ) the particle projection area, ( $C_D$ ) the drag coefficient, and ( $x$ ) the particle position, calculated from the location where it enters the jet (shown as  $x = 0$  in Figure 1). The relative velocity between particle and gas ( $V_g - V_p$ ) is multiplied by its absolute value to maintain the appropriate direction of the drag force for cases where the particle is moving faster or slower than the gas. The drag coefficient ( $C_D$ ) is a function of the gas Reynolds number which for the range of validity  $Re_g = 0.2 - 500$  is in the form [13]:

$$C_D = \left( \frac{24}{Re_g} \right) \left( 1 + \frac{3}{16} Re_g \right)^{\frac{1}{2}}, \quad (2)$$

This correlation was based on the assumption that the particles before the impact were spherical, which is consistent with assumptions made in the heat transfer predictions and

impact modeling. The Reynolds number for the relative gas flow around a particle of diameter (D) is defined as:

$$\text{Re}_g = \rho_g \frac{|\mathbf{v}_g - \mathbf{v}_p|}{\mu_g} D, \quad (3)$$

A high Biot number of a polymer particle in an HVOF jet implies that particles are likely to develop significant temperature gradients between the core and the surface and the particle temperature should not be modeled as uniform. Accordingly, the equations describing the heat transfer from the gas to a single spherical particle (assuming spherical symmetry) with appropriate initial and boundary conditions are as follows:

$$\rho_p C_{p_p} \frac{\partial T_p}{\partial t} = \frac{1}{r^2} \frac{\partial}{\partial r} \left( r^2 k_p \frac{\partial T_p}{\partial r} \right), \quad (4)$$

$$T_p(r, t = 0) = T_p^0$$

$$\frac{dT_p}{dr}(r = 0, t) = 0, \quad -k_p \frac{dT_p}{dr}(r = R_p) = h(T_p(R_p) - T_g),$$

where ( $T_p$ ) is the particle temperature, and ( $\rho_p$ ), ( $C_{p_p}$ ), and ( $k_p$ ) are the density, heat capacity and thermal conductivity of the particle, ( $r$ ) is radial distance from the centre of the particle, ( $R = D/2$ ) is particle radius and ( $h$ ) is the heat transfer coefficient. The heat transfer coefficient, ( $h$ ), is computed by the Ranz-Marshall semi-empirical equation [14]:

$$\frac{h D}{k_g} = \text{Nu} = 2 + 0.65 \text{Re}_g^{1/2} \text{Pr}_g^{1/3}, \quad (5)$$

where ( $\text{Nu} = h D/k_g$ ) is the Nusselt number and ( $\text{Pr}_g = C_{p_g} \mu_g / k_g$ ) is the Prandtl number.

The equations (Equations 1 - 4) for momentum and heat transfer were solved by numerical integration using the Forward Euler method with a time step small enough ( $10^{-7}$  s) that the local Reynolds number, gas velocity and temperature could be considered constant over each time step.

### 2.3 Particle Impact and Spreading

Impact and deformation of thermally sprayed droplets on a rigid surface are characterized by the complex three-dimensional large deformation of free surfaces. The splashing droplet typically is not axisymmetric which would require a three-dimensional model for realistic splat predictions. Three dimensional, highly irregular, free surface flows including creation of new surfaces have been commonly solved using fixed grid Eulerian-boundary tracking methods (e.g. volume of fluid methods (VoF) [15]) such as the one used in this paper, Flow-3D<sup>®</sup> (version 9.0). This VoF method utilizes a fixed-grid volume tracking algorithm to track the fluid deformation and the droplet free surface based on the fluid fraction function defined to be equal to one in the fluid and zero outside the fluid. The computational domain including fixed grid and a schematic representation of initial and boundary conditions used in this paper is shown in Figure 2.

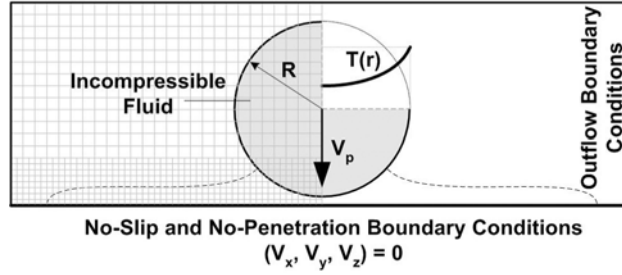


Figure 2. Boundary conditions, initial conditions and cross-section of a typical mesh used in Flow3D®.

In our model, we neglected solidification, heat transfer from splat to substrate and capillary effects which all were proven to have secondary effects on spreading of a molten polymer droplet [16]. The viscosity of molten polymer droplet is modeled considering both shear thinning and temperature dependence ( $\mu(\dot{\gamma}, T)$ ) using the Carreau model [17] in the form:

$$\mu = \mu_{\infty} + \frac{\mu_0 E_T - \mu_{\infty}}{\left[1 + (\lambda E_T)^2 \dot{\gamma}^2\right]^{\frac{1-n}{2}}}, \quad (6)$$

where the temperature component is:

$$E_T = \exp\left[a\left(\frac{T^*}{T-b} - c\right)\right] \quad (7)$$

where ( $\mu_{\infty} = 0$ ) and ( $\mu_0 = 13000$  poise at  $T^* = 240$  °C) are infinite shear-rate and zero shear-rate viscosities, respectively, ( $\lambda = 1$ ) is a time constant, ( $n = 0.7$ ) is the “power-law exponent” and ( $a = 16$ ), ( $b = 0$ ) and ( $c = 1$ ) are constants for the temperature dependence. All curve-fitting coefficients in Carreau model were determined based on experimental viscosity data. The three dimensional spreading progression at characteristic dimensionless times ( $t^* = t/(D/V_p)$ ) was generated for 30, 60, 90 and 120  $\mu\text{m}$  particles. These particle sizes were chosen to cover the particle size range of the as-received nylon 11 powder used for HVOF spraying and in our experiments as detailed in the next section.

### 3. Experiments

Semicrystalline Polyamide (nylon 11) powder commercially available as Rilsan PA-11 French Natural ES D-60 (donated by Arkema, Inc.) was used as the feedstock for the thermal spray experiments reported. The as-received powder had a mean particle size of 60  $\mu\text{m}$ . The melting and degradation temperatures of nylon 11, as reported by the manufacturer, were in the range 182 - 191 °C and 357 - 557 °C, respectively.

Swipe or “splat” tests were conducted by single high speed ( $> 0.7$  m/s) spray passes across *room temperature* glass slides at low powder feed rates ( $\sim 2$  g/min). Splat tests were used to observe the morphology of individual splats. Splat tests were carried out using the Stellite Coatings, Inc. Jet-Kote II® HVOF spray system (Figure 1) using an Oxygen and Hydrogen flow rates of 0.0024/0.0039  $\text{m}^3/\text{s}$  (300/500 scfh), respectively and spray distance of 225 mm. The spray nozzle used was 150 mm long with an internal diameter of 6.4 mm. The splat morphologies were analyzed using optical microscopy (Olympus PMG-3 optical metallograph).

In-flight particle velocities at a distance of 100 mm from the nozzle exit were measured using a *SprayWatch 2i* system in conjunction with a diode laser illumination source, both provided by Oseir Ltd. from Tampere, Finland. The measurements were conducted at Oxygen and

Hydrogen gas flow rates of 300 and 500 scfh, respectively (a total gas flow rate of 1.86 g/s at  $\Phi = 0.83$ ) the same parameters used for coating and splat deposition. The number of particles recorded was 306.

One of the important characteristics of thermal spraying in general is a relatively large number of process parameters that need to be controlled during the spray process. Although this is often challenging in respect to process repeatability, it also increases the number of parameter combinations that can be varied in order to achieve specific coating properties. The HVOF spray parameters used in these experiments were chosen as a base line case to be used as reference for numerical model development.

## 4. Results and Discussion

The results of the three key modeling steps considered in this paper, including particle acceleration and heating in an HVOF jet and particle spreading upon impact with a substrate, are presented in the following sections. The experimental observations used to support and evaluate the accuracy of numerical models are summarized in the next section.

### 4.1 Experimental Observations

A critical link for better understanding the relationship between HVOF process parameters and coating microstructure is the individual splat formation process as the unit building block. The morphology of nylon 11 splats deposited in a swipe test onto room temperature glass slides are shown in Figures 3. When the substrate was at room temperature, most of the larger splats ( $> 100 \mu\text{m}$ ) exhibited a characteristic “fried-egg” shape with a large, nearly-hemispherical, core in the centre of a thin disk. This shape indicated the existence of a large radial difference in the flow properties of the molten surface of nylon 11 droplets and the largely unmelted core; i.e. the “fried-egg” shaped splats were formed by polymer particles having a large radial temperature profile – a low temperature, high viscosity core and a high temperature, low viscosity surface.

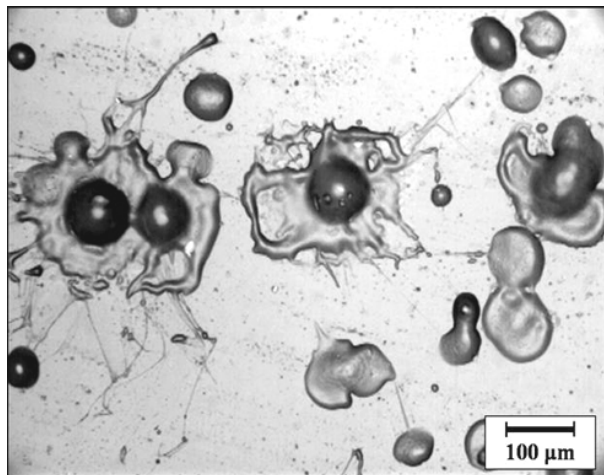


Figure 3. Nylon-11 splats deposited via a swipe test onto a room temperature glass slide.

### 4.2 Particle Velocity

The acceleration of particles in the HVOF jet was predicted by solving equations (1) – (3), and the results are displayed in Figure 4. The predicted velocities of 30, 60, 90 and 120 μm particles at the moment of impact on the substrate (spray distance of 225 mm) were 537, 497, 427 and 368 m/s. In general, polymer particles accelerate much faster than similar size metallic or cermet particles in HVOF jets [11, 12]. This is due to much lower density of

polymers ( $0.9 - 1.4 \text{ g/cm}^3$ ) versus metals or cermets ( $\sim 2.7 - 15 \text{ g/cm}^3$ ). For the same reason, polymer particles have lower inertia and their velocity responds more rapidly to the decreasing gas velocity after exiting the gun nozzle.

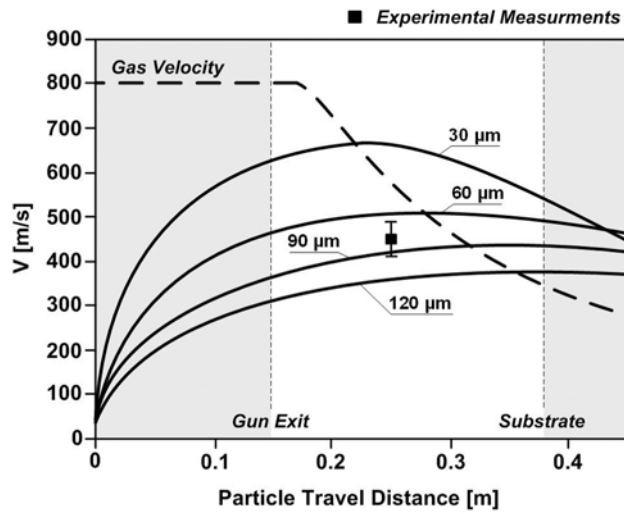


Figure 4. Predicted particle and gas velocities combined with experimental measurements at the spray distance of 100 mm after the gun exit.

The results of the in-flight particle velocity measurements carried out using the *SprayWatch 2i* system were combined with numerical velocity predictions in Figure 4. Mean particle velocity 100 mm after the gun exit was 433 m/s with a standard deviation of 20 based on a count of 306 particles. The measured particle velocities compared well with predicted velocities of 60 - 90  $\mu\text{m}$  particles. This was expected since this particle size range covers  $\sim 70\%$  of the total nylon 11 feedstock volume used for the experimental measurements.

### 4.3 Particle Heating

The heat transfer from the combusting gas to the nylon 11 particles was predicted by solving equations (4) and (5) simultaneously with the momentum transfer equations (1) – (3) for particle acceleration in HVOF jet. The temperature profiles within 30, 60, 90 and 120  $\mu\text{m}$  diameter particles immediately before impact with a substrate are displayed in Figure 5.

Forced convection from the HVOF jet to a micron size particle is characterized by a high convective heat transfer coefficient ( $h \sim 5000 - 17000 \text{ W/(m}^2\text{K)}$ ). Despite the rapid rise in surface temperature, the high internal thermal resistance (high Bi number) of nylon 11 particles prevents the interior of the particle from being heated at the same rate. As a result, a 90  $\mu\text{m}$  particle develops a large temperature gradient between the core and its surface. The core region ( $< 36 \mu\text{m}$ :  $r/R = 0.4$ ) is below the nylon 11 melting temperature ( $182 - 191 \text{ }^\circ\text{C}$ ) while the surface region ( $> 77 \mu\text{m}$ :  $r/R = 0.85$ ) has a temperature exceeding the upper degradation limit of  $560 \text{ }^\circ\text{C}$ . Similarly, a 120  $\mu\text{m}$  particle had an unmelted core and surface temperature above the degradation temperature, whereas a 60  $\mu\text{m}$  particle was fully melted, but with almost 50% of its volume above the degradation temperature. The temperature of a 30  $\mu\text{m}$  particle under present HVOF conditions was more than twice as high as the upper degradation limit, indicating that such small particles will most likely be fully degraded during spraying.

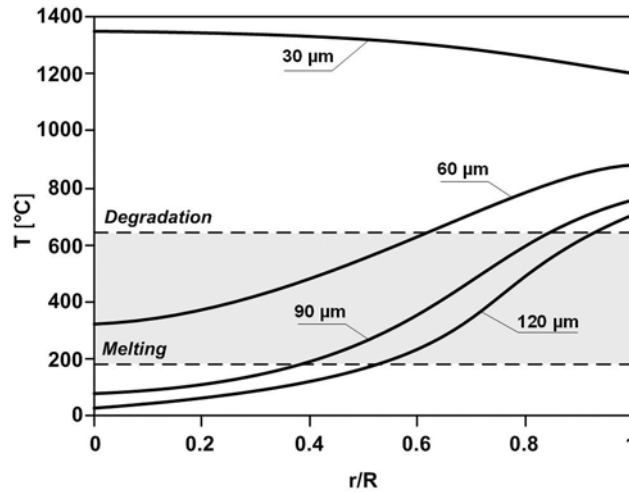


Figure 5. Particle temperature profiles within nylon 11 particles immediately before impact with a substrate at 225 mm spray distance.

According to numerical predictions, particles smaller than  $\sim 40 \mu\text{m}$  and the surfaces of larger particles exceed the nylon 11 degradation temperature under present spray conditions. The particles, however, spend a very short time under these conditions ( $\sim 0.7 - 1.5 \text{ ms}$ ). A better understanding of potential polymer degradation during HVOF spray process and accurate mathematical predictions require a consideration of the polymer's degradation kinetics. This topic is beyond the scope of this paper and it will be treated as a separate subject. In the following section, the predicted temperature profiles inside the particles will be used as initial condition for impact and deformation model as they are presented in Figure 5, assuming that no degradation occurs.

#### 4.4 Particle Deformation

The shear rate and temperature dependent viscosity of nylon 11, predicted using the Carreau model (Equations 6 and 7) and used for three-dimensional splat predictions, is shown in Figure 6. In our model solidification of the droplet is modeled only through a temperature dependent viscosity. The portion of the droplet below the melting temperature ( $< 182 \text{ }^\circ\text{C}$ ) was still considered liquid, however, with a viscosity sufficiently high ( $> 10^4 \text{ poise}$ ) (Figure 6) so that it would not deform significantly on impact.

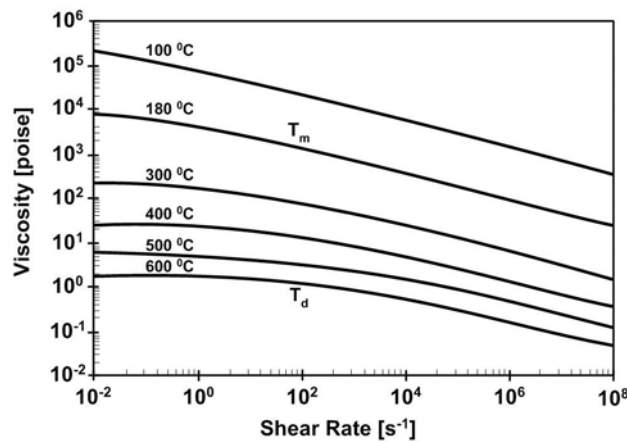


Figure 6. Shear rate and temperature dependent viscosity of nylon 11 predicted using Carreau model (Equations 13 and 14).

Particle impact velocity (Figure 4), temperature profile with neglected polymer degradation (Figure 5) and temperature and shear rate dependent viscosity (Figure 6) were all combined together as a part of three-dimensional deformation model, the results of which are displayed in Figure 7. The predicted splat shapes shown in Figure 7 exhibited a good qualitative comparison with the experimentally observed splat shapes shown in Figure 3. The larger, 90 and 120  $\mu\text{m}$  particles were spread into “fried egg” splats with large nearly-hemispherical cores in the centers of a thin disk, whereas 30 and 60  $\mu\text{m}$  particles generated flattened splats with small elevation in the centre. This was consistent with the predicted internal temperature profiles, since both the 90 and 120  $\mu\text{m}$  diameter particles had unmelted cores as shown earlier in Figure 5. In addition a larger unmelted portion of the 120  $\mu\text{m}$  diameter particle transformed into a larger central “dome” than for a splat arising from a 90  $\mu\text{m}$  diameter particle. Both 30 and 60  $\mu\text{m}$  particles generated rims with breakup and satellites radiating from the splat edge. This was expected since smaller particles have higher temperature and lower viscosity around their surface.

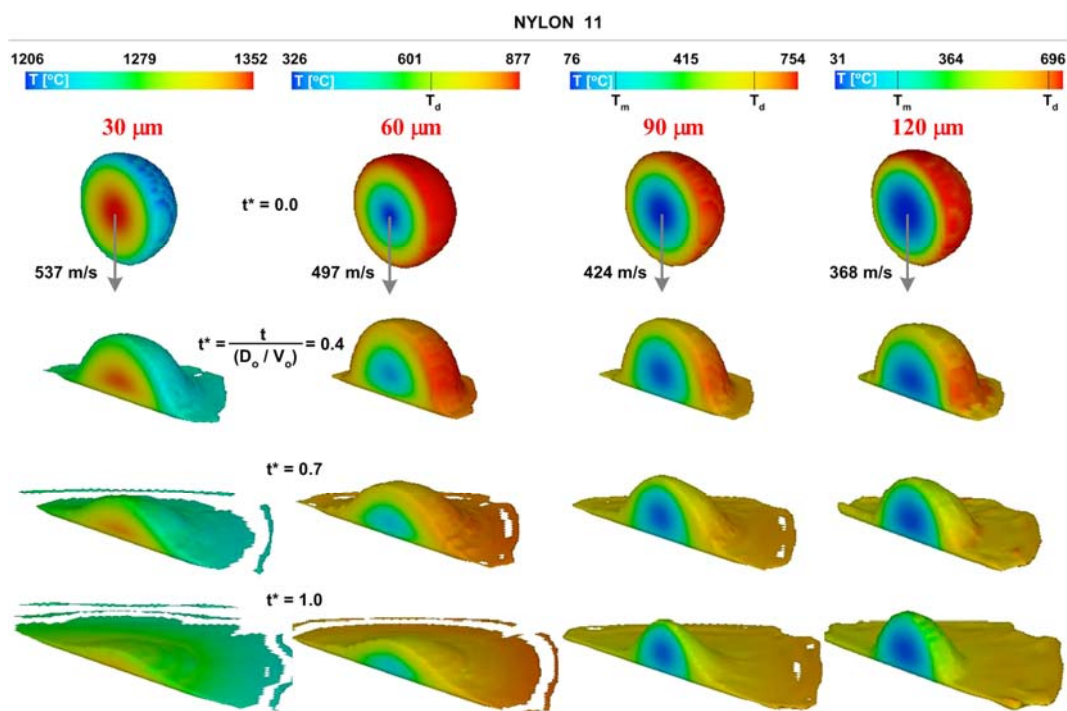


Figure 7. Cross-sections of predicted three-dimensional spreading splats for 30, 60, 90 and 120  $\mu\text{m}$  diameter particles. Colors indicate the internal temperature distribution.

## 5. Conclusions

One of the principal goals of this work was to develop a knowledge base and improved qualitative understanding of the transport and impact behavior of polymeric particles in the HVOF combustion spray process. Mathematical models of (1) the acceleration, (2) the heating and (3) the deformation of nylon 11 particles were developed. Heating and acceleration are fully coupled and calculated within the same FORTRAN code. Results from the particle heating and acceleration computations were used as the initial conditions for modeling the particle deformation on impact with a substrate by Flow-3D<sup>®</sup> computational fluid dynamic software.

Molten nylon 11 was modeled as a generalized Newtonian fluid with temperature and shear rate dependent viscosity. The predictions showed that larger polymer particles (i.e. 90 - 120  $\mu\text{m}$ ) develop steep internal temperature gradients between the core and the surface during HVOF spraying. The prediction was in agreement with experimental observations of thermally sprayed splats, since most large nylon 11 splats sprayed onto a room temperature substrate

exhibited a “fried-egg” shape. This shape is likely formed by polymer particles having a low temperature, high viscosity core and a high temperature, low viscosity surface. Theoretical predictions and experiments presented in this paper indicate that the HVOF combustion spray process is a viable method for the solvent-free deposition of polymers. The models also pointed out several important process drawbacks, such as overheating of small particles (i.e. < 40  $\mu\text{m}$ ) and incomplete melting of larger particles (i.e. > 70  $\mu\text{m}$ ). Addressing these issues may not only help to improve the understanding of the relationships between processing conditions, splat morphology and coating microstructure of HVOF sprayed polymer coatings but also help with the development of a new low temperature thermal spray process. An optimal thermal spray process for polymers should utilize a low gas temperature (~ 100 - 500  $^{\circ}\text{C}$ ) to prevent overheating of the polymer particles, a high gas velocity to provide high kinetic energy for spreading of the high melt viscosity particles and a sufficiently long dwell time for uniform particle melting.

## Acknowledgments

The authors would like to thank the National Science Foundation (NSF) for providing support for this research under a collaborative research grant, number DMI 0209319. The views expressed in this paper do not necessarily reflect those of NSF. The authors would like to thank Arkema Corporation for donating the nylon 11 powders used in this work.

The authors also greatly appreciate the assistance of Mr. Dustin Doss during the HVOF spraying of the coatings and help of Dr. Thomas E. Twardowski and Mr. Varun Gupta during results analysis.

## References

1. Davis, J. R., (Ed.) et al, 2004, *Handbook of Thermal Spray Technology*, ASM International®, 1<sup>st</sup> Ed., Materials Park, OH.
2. Fauchais, P., Vardelle, A., Dussoubs, B., 2005, Quo Vadis Thermal Spraying?, *J of Thermal Spray Technology*, **10(1)**, pp. 44 – 66.
3. Zhang, T., Gawne, D. T., Bao, Y., 1997, The Influence of Process Parameters on the Degradation of Thermally Sprayed Polymer Coatings, *Surface and Coating Technology*, **96**, pp 337 – 344.
4. Brogan J. A. and Berndt C. C., 1997, The Coalescence of Combustion-Sprayed Ethylene-Methacrylic Acid Copolymer, *Journal of Materials Science*, **32**, pp. 2099 - 2106.
5. Petrovicova E, Knight R, Schadler LS, Twardowski TE, 2000, Nylon 11/silica nanocomposite coatings applied by the HVOF process. I. Microstructure and morphology,” *Journal of Applied Polymer Science*, **77 (8)**, pp. 1684-1699.
6. Petrovicova, E., Schadler L. S., 2002, Thermal Spray of Polymers, *International Materials Review*, **47**, (4), pp. 169-190.
7. Ivosevic, M., Knight, R., Kalidindi, S. R., Palmese G. R., and J. K. Sutter, 2005, Adhesive/Cohesive Properties of Thermally Sprayed Functionally Graded Coatings for Polymer Matrix Composites, *Journal of Thermal Spray Technology*, **14(1)**, pp. 45 – 51.
8. Sobolev, V. V., Guilemany J. M., 1999, Flattening of Droplets and Formation of Splats in Thermal Spraying: A Review of Recent Work-Part 1, *Journal of Thermal Spray Technology*, **8 (1)**, pp. 87 - 101.

9. Fauchais, P., Fukumoto, M., Vardelle, A. and Vardelle, M., 2004, Knowledge Concerning Splat Formation: An Invited Review," *Journal of Thermal Spray Technology*, **13 (3)**, pp. 337 - 360.
10. Dobbins, T. A., Knight, R. and Mayo, M. J., 2003, HVOF Thermal Spray Deposited  $Y_2O_3$ -Stabilized  $ZrO_2$  Coatings for Thermal Barrier Applications, *Journal of Thermal Spray Technology*, **12 (2)**, pp. 214 - 225.
11. Tawfik, H. H. and Zimmerman, F., 1997, Mathematical Modeling of the Gas and Powder Flow in HVOF Systems," *Journal of Thermal Spray Technology*, **6 (3)**, pp.345 - 352.
12. Cheng, D., Trapaga, G., McKelling, J. W. and Lavernia, J. E., 2001, Mathematical Modeling of High Velocity Oxygen Fuel Thermal Spraying: An Overview," *Key Engineering Materials*, **197**, pp.1 -26.
13. Douglas, J. F., Gasiovek, J. M., Swaffield, J. A., 1995, Fluid Mechanics, 3<sup>rd</sup> Ed., Longman Group Limited.
14. Bird, R. B., Stewart, W. E., and Lightfoot, E. N., 1960, Transport Phenomena, Wiley, New York, USA.
15. Hirt, C. W. and Nichols, B. D., 1981, Volume of Fluid (VoF) Method for the Dynamics of Free Boundaries, *Journal of Computational Physics*, **39**, pp. 201 - 225.
16. Ivosevic, M., Cairncross, R. A. and Knight, R., 2004, Heating and Impact Modeling of HVOF Sprayed Polymer Particles, *Proc. 2004 International Thermal Spray Conference [ITSC-2004]*, DVS/IIW/ASM-TSS, Osaka, Japan.
17. Bird, B. R., Armstrong, R. C. and Hassager, O., 1987, Dynamics of Polymeric Liquids, Volume 1: Fluid Mechanics, 2<sup>nd</sup> Ed., John Wiley & Sons, Inc.